Accelerated Publications

Metal Binding and Oxidation of Amyloid-β within Isolated Senile Plaque Cores: Raman Microscopic Evidence[†]

Jian Dong,[‡] Craig S. Atwood,[§] Vernon E. Anderson,[‡] Sandra L. Siedlak,[§] Mark A. Smith,[§] George Perry,[§] and Paul R. Carey*,[‡]

Department of Biochemistry and Department of Pathology, School of Medicine, Case Western Reserve University, 10900 Euclid Avenue, Cleveland, Ohio 44106

Received November 20, 2002; Revised Manuscript Received December 10, 2002

ABSTRACT: Alzheimer's disease (AD) is characterized by the deposition of amyloid plaques in the parenchyma and vasculature of the brain. Although previous analytical studies have provided much information about the composition and structure of synthetic amyloid-β fibrils, there is, surprisingly, a dearth of data on intact amyloid plaques from AD brain. Therefore, to elucidate the structure and detailed composition of isolated amyloid plaque cores, we utilized a high-resolution, nondestructive technique, Raman microscopy. The data are of very high quality and contain detailed information about protein composition and conformation, about post-translational modification, and about the chemistry of metal binding sites. Remarkably, spectra obtained for senile plaque (SP) cores isolated from AD brain are essentially identical both within and among brains. The Raman data show for the first time that the SP cores are composed largely of amyloid-β and confirm inferences from X-ray studies that the structure is β-sheet with the additional possibility that this may be present as a parallel β-helix. Raman bands characteristic of methionine sulfoxide show that extensive methionine oxidation has occurred in the intact plaques. The Raman spectra also demonstrate that Zn(II) and Cu(II) are coordinated to histidine residues in the SP cores, at the side chains' N_τ and N_π atoms, respectively. Treatment of the senile plaques with the chelator ethylenediaminetetraacetate reverses Cu binding to SP histidines and leads to a broadening of amide features, indicating a "loosening" of the β-structure. Our results indicate that Aβ *in vivo* is a metalloprotein, and the loosening of the structure following chelation treatment suggests a possible means for the solubilization of amyloid deposits. The results also reveal a direct chemical basis for oxidative damage caused by amyloid-β protein in AD.

Neurodegenerative diseases are defined pathologically by the aggregation of protein in deposits such as senile plaques (SPs),[1] neurofibrillary tangles, Lewy bodies, Pick's bodies, and Hirano bodies. Compositional analyses have shown that SP cores in AD consist of Aβ (*1*−*3*) and numerous other associated protein and nonprotein components (reviewed in ref *4*). The relative contribution of these components to amyloid deposits and the structural characteristics of SP cores, however, remain unknown. Limited structural information has been obtained for SP; electron microscopic studies indicate that fibrils from the plaques are 4−8 nm in diameter and composed of two 2−4 nm filaments (*5*), and X-ray fiber diffraction has claimed a β-pleated sheet structure with repeat distances in the fibers at 4.8 and 10.6 Å (*6*). Both SP *in situ* and synthetic Aβ fibrils *in vitro* display birefringence in polarized light when stained with Congo red (*7*) and fluorescence when bound with thioflavin T. These data indicate an ordered protein structure in the SPs (*8*) and led to the assumption that SP cores have the same secondary structure (repeating, antiparallel cross β-pleated sheet) as proposed for most synthetic Aβ fibrils.

Most of the conclusions about the composition and structure of intact SP cores are inferential and are based on analogy to synthetic Aβ fibers. The reason for this is easily understood; there are almost no techniques available that provide "hard" structural and chemical data on individual biological assemblies with dimensions in the 5 μm range. In this paper, we demonstrate that Raman microscopy, which combines optical microscopy with a Raman spectrograph, meets this need. High-quality Raman spectra have been obtained from SP cores. The interpretation of the Raman data is based on the work of a number of laboratories in the bio-Raman/protein field in the past 30 years. In particular, Takeuchi, Miura, and co-workers (*9*−*12*) have recently

[†] This study was supported by the National Institutes of Health (Grants AG 14249 to G.P. and V.E.A., AG 19536 to C.S.A., and GM 54072 to P.R.C.) and the Alzheimer's Association (Grant IIRG-00-2163 to M.A.S.).

* To whom correspondence should be addressed. Telephone: (216) 368-0031. Fax: (216) 368-3419. E-mail: carey@biochemistry.cwru.edu.

[‡] Department of Biochemistry.

[§] Department of Pathology.

[1] Abbreviations: AD, Alzheimer's disease; SP, senile plaque; Aβ, amyloid-β; EDTA, ethylenediaminetetraacetate; PBS, phosphate-buffered saline.

10.1021/bi0272151 CCC: $25.00
Published on Web 02/20/2003

undertaken seminal studies using Raman spectroscopy to characterize metals binding to synthetic Aβ and to peptides derived from Aβ. They have built a library of spectra−structure correlations for Zn(II) and Cu(II) binding to different sites on the histidine side chain (*10*, *13*−*15*) and have confirmed earlier spectral markers for transition metals binding to tyrosinate (*16*). We have been able to use these correlations to detect and monitor metal binding sites in intact SP cores to provide the first information that pertains to an *ex vivo* situation. This information, together with the Raman evidence for methionine oxidation, provides support for proposals that this species and Cu-bound histidine are involved in the generation of neurotoxic H_2O_2.

EXPERIMENTAL PROCEDURES

Senile Plaque Core Isolation and Amyloid-β Characterization. SP cores were isolated from cortical gray matter from patients with pathologically confirmed Alzheimer's disease ($n = 3$; 76, 81, and 94 years old) as described previously (*17*). After purification, they were separated using a fluorescence-activated cell sorter (FACS) to select 5−35 μm particles from smaller and larger fractions and further into two populations displaying bright and dull autofluorescence. Aliquots of the sorted fractions were dried on a glass slide, stained with Congo red, viewed under cross-polarized illumination, and determined by manual counting to be >90% pure. Aliquots of purified amyloid cores were suspended in PBS and dried on either aluminum foil or silver foil for Raman analysis. In the chelation tests, the deposited core samples were soaked in a 2.5 mM EDTA (adjusted to pH 7.0) solution in a tightly sealed container for 24 h, and analyzed by Raman microscopy after redrying.

In addition to displaying morphological characteristics and Congo red birefringence, the purified cores also were analyzed immunocytochemically (*18*) for amyloid content. The purified cores were dried on a glass microscope slide, immunostained using monoclonal antibody 498, and developed using standard peroxidase anti-peroxidase methods.

Human Aβ(1−42) was synthesized and purified by HPLC and characterized by amino acid analysis and mass spectroscopy by the W. M. Keck Foundation Biotechnology Resource Laboratory (Yale University, New Haven, CT). Aβ(1−42) was identified as a single peak upon HPLC and showed no chemical modification. Aβ fibrils were generated by dissolving Aβ(1−42) (1 mg/mL) in doubly deionized water for 2 days at 37 °C.

Raman Spectroscopy. SP core and Aβ fibril samples were placed in the focused laser beam with the help of a Raman microscope system, as described previously (*19*). Ten milliwatts of 647.1 nm laser excitation from a krypton laser was used to generate the Raman scattering under a 100× objective with a data acquisition time of 1 min.

RESULTS AND DISCUSSION

To examine the structural features of SP, cores were isolated from AD brains ($n = 3$) following homogenization of hippocampal tissue, fractionation by sucrose gradient, and then sorting via size using flow cytometry. SP cores isolated in this manner and treated with Congo red displayed birefringence under polarized light (Figure 1a) and were immunopositive for Aβ specific antibodies (Figure 1b).

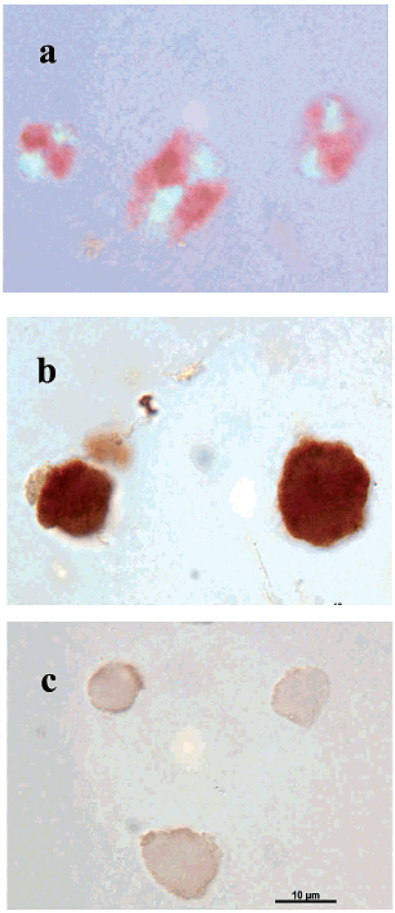

FIGURE 1: Senile plaque (SP) cores purified from brain demonstrate characteristic Congo red birefringence under polarized light (a) and are strongly reactive with antisera to Aβ(1−42) (b) but not with irrelevant antisera (c). The scale bar is 10 μm.

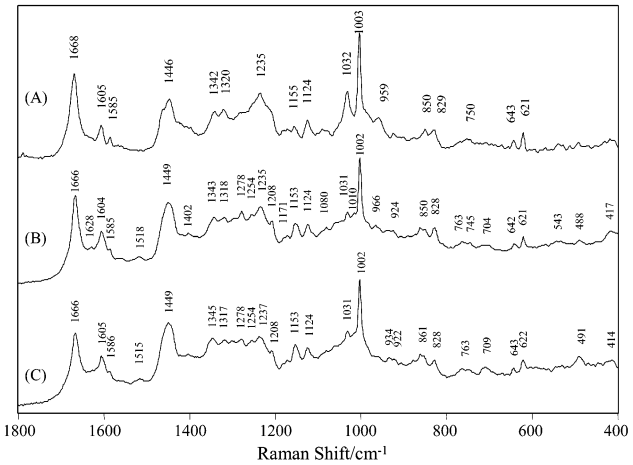

FIGURE 2: Raman spectra of (A) synthetic Aβ(1−42) fibrils, (B) SP cores, and (C) SP core treated with 2.5 mM EDTA (pH 7.0) for 24 h.

SP Cores: Composition and Protein Conformation. Comparison of the Raman spectra of SP cores with synthetic Aβ fibrils (Figure 2; Table 1 lists assignments for the major bands) indicates the protein compositions of these samples are similar. The equivalence of the Raman profiles is evidenced by (i) the similar relative intensities of the "sharp" ring modes identified for both Phe and Tyr side chains in SP cores and Aβ fibrils suggesting the same composition for these amino acids; (ii) the similarity in the profiles of

Table 1: Raman Frequencies and Assignments for SP Cores

frequency (cm^{-1})	assignment[a]
1666	amide I in β-sheet
1628	C═O bound to metal
1604	[Zn−histidine], Phe, Tyr^-
1585	Phe
1518	unknown
1449	CH_2 scissor, CH_3 deformation
1402	COO^- symmetric stretch in Asp, Glu
1343	[Cα−H bend + Cα−C stretch] + CH_2 twist/wag
1318	amide III and CH_2 twist/wag
1295 (shoulder)	Zn−histidinate
1278	Cu−histidine
1254	amide III disordered
1235	amide III in β-sheet
1208	Tyr, Phe
1171	Tyr, Phe
1160 (unresolved)	Val, Ile
1153	[C−N] + Ile
1124	Val, Ile + [C−Cα and C−N stretch]
1080	[C−C and C−N stretch], Lys, Arg, Gln, Asn
1031	Phe
1010	S═O, methionine sulfoxide
1002	Phe
966	CH_2 symmetric rock + C−Cα
861	unknown
850	Tyr
829	Tyr
763	Ala
704−710	methionine sulfoxide
642	Tyr
621	Phe

[a] Assignments are based on refs *20*, *24*, and *44*.

the bands emanating from the aliphatic side chains; (iii) the absence of the characteristic and easily identifiable narrow bands for Trp (near 1555 and 760 cm^{-1}; Aβ contains no Trp) in SP cores; and (iv) the absence of a "group frequency" for a S−S stretch that occurs for disulfide-bearing proteins near 510 cm^{-1}. These results provide strong evidence that SP cores are composed primarily of Aβ, and suggest that other proteins previously localized to amyloid plaques by immunocytochemistry (*4*) are primarily peripheral to the core amyloid, or are present in minor amounts.

Comparison of the Raman spectra of synthetic Aβ(1−42) fibrils (Figure 2A) with SP cores (Figure 2B) also provides compelling evidence that the secondary structure of the major component of the cores resembles strongly that of synthetic Aβ fibrils. Conformation-sensitive amide I and amide III regions are essentially the same for the Aβ(1−42) fibrils when compared with the SP cores. The amide I bands occur at 1668 and 1666 cm^{-1}, with bandwidths at half-height of 23 and 22 cm^{-1} for the Aβ fibrils and SP cores, respectively. The position and relatively narrow band profiles connote very similar and highly ordered β-type structures (*20*). This is reinforced by the distinctive amide III bands at 1235 cm^{-1} identified in both samples that are highly characteristic of a β-structure. The amide I and III profiles in Figure 2B also bear remarkable resemblance to those for the P22 tail-spike protein, a protein of known parallel β-helix conformation (*21* and references therein), suggesting that the Aβ fibrils and SP cores are also parallel β-helices. This conclusion also conforms to the prediction of Blake and co-workers (*22*; for a recent review, see ref *43*), who proposed that amyloid fibrils are made up of β-sheet helices and recent solid state NMR data for synthetic Aβ fibrils that are consistent only with a parallel β-structure (*23*). In general, the Raman profile in the spectral range of 1200−1400 cm^{-1} is sensitive to protein conformation. When slight differences in spectral resolution are taken into account, this profile is very similar for Aβ fibrils and SP bodies, offering further evidence for equivalent protein conformations. One exception, discussed below, is the peak seen only in the SP samples at 1278 cm^{-1}. There is no evidence in the Raman spectra for a significant population of peptide bonds in α-helical space (e.g., intensity near 1655 cm^{-1} in the amide I region). However, the low-intensity band/shoulder at 1254 cm^{-1} in parts A and B of Figure 2 may arise from a minor segment of the protein chains being in an unordered region.

Our conclusion that SP cores are made up primarily of Aβ in β-type structures is consonant with the views of most researchers in the field. However, it is worth noting that in the X-ray fiber diffraction evidence for β-structure the signal-to-noise ratio is no better than 2:1 tenuous (*6*) and the protein composition in the plaques has never been quantitated. Thus, the Raman microscope data provide the best structural and microchemical characterization of SP cores.

Chemistry of Amino Acid Side Chains in SP Bodies. (1) Glutamic and Aspartic Acids. Aβ contains three Asp and three Glu residues, and all appear to be ionized in the SPs. A Raman feature near 1402 cm^{-1} is due to the COO^- symmetric stretch from acid side chains, and this and the lack of a discernible feature for the COOH group near 1720 cm^{-1} indicate that most, if not all, the acid side chains are deprotonated (Figure 2).

(2) Tyrosine. Aβ contains one Tyr residue, and in the SP core protein, it appears to be present predominantly as tyrosinate, i.e., the O^- form. The evidence is provided by the intensity ratio of the "tyrosine doublet" at 850/830 cm^{-1}, which is slightly less than 1 and is symptomatic of tyrosinate (*24*). Precise quantitation of the doublet ratio is rendered difficult by the presence of a feature, of unknown origin, in Figure 2B near 860 cm^{-1}. The secondary evidence is the absence of a feature at 1618 cm^{-1} that is characteristic of the tyrosine side chain in its OH form (*24*). However, the 1618 cm^{-1} band may be difficult to detect since we do not see it for the model protein (Figure 2A), where the single tyrosine is almost certainly in its neutral form. In Figure 2A, the tyrosine doublet ratio is close to 1, providing evidence for the side chain in its OH form. Note, in the SP cores, we find no evidence for tyrosinate−Fe or −Cu binding (below).

(3) Methionine. To set up reference Raman data for the oxidation of methionine side chains, we recorded the Raman spectra of 30 mM L-methionine in an aqueous solution and of 30 mM methionine treated with 5% H_2O_2 for 3 h. The latter treatment produces the "sulfoxide form" of the side chain. The spectra in Figure 3 show that oxidation to the sulfoxide results in the appearance of relatively intense Raman bands near 1419, 1010, and 704 cm^{-1}. The latter two are assigned to the S═O stretch from the methionine sulfoxide in a hydrogen-bonded environment and to the C−S stretches from methionine sulfoxide, respectively. These modes assume importance since they are in regions that offer the potential for marker bands. Interestingly, there is no evidence for bands near 1010 and 704 cm^{-1} in the synthetic fibrils (Figure 2A), but they do occur in the spectra of the SP cores (Figure 2B). This is strong evidence that extensive side chain oxidation has occurred in the sole methionine of the Aβ protein within the SP cores. The

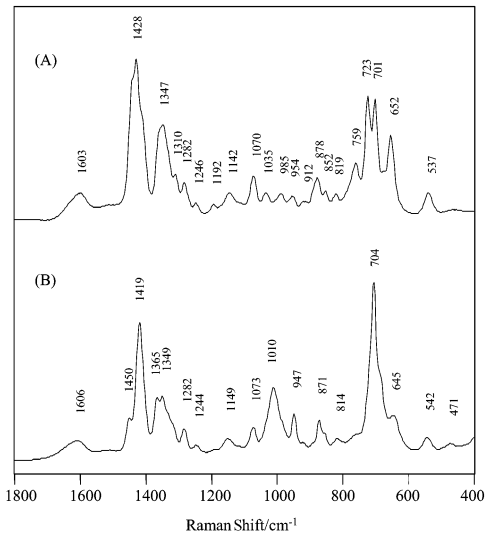

FIGURE 3: Raman spectra (A) of 30 mM L-methionine in an aqueous solution and (B) of 30 mM methionine treated with 5% H_2O_2 for 3 h. Both were recorded in 150 mM KP_i buffer (pH 7.15) with the buffer spectrum subtracted.

presence of methionine sulfoxide is consistent with reports that methionine is critical for oxidation/reduction reactions in the peptide (*25*), and this is discussed further below.

We note that a few bands in the spectrum of the untreated cores (Figure 2B) have not been assigned in Table 1, namely, 1518 (broad), near 1150, and 861 cm^{-1}; these may arise from chemically modified amino acid side chains, or from relatively small amounts of unidentified nonprotein components.

Metal Binding to Aβ in the SP Cores. Cu(II), Zn(II), and Fe(III) have been reported to be enriched in amyloid plaques in AD (*26*). *In vitro*, synthetic Aβ possesses selective high- and low-affinity Cu(II) and Zn(II) binding sites that mediate its protease resistance, reversible precipitation (*27*−*29*), and the O_2-dependent production of H_2O_2 and concomitant toxicity (*30*−*32*). However, direct evidence for a metal ion binding configuration in Aβ within SPs has not been demonstrated.

Several differences seen between the Raman spectra of synthetic Aβ fibrils (Figure 2A) and SP cores (Figure 2B) can be ascribed to vibrational modes arising from metal ions bound to the SP protein. Our interpretation of these data is greatly assisted by the pioneering work of Takeuchi, Miura, and co-workers on the Raman studies of metals binding to synthetic Aβ and peptide fragments derived from Aβ. On the basis of their model studies (*9*, *10*), increased intensity at 1604 cm^{-1} in SP cores compared with Aβ fibrils (by approximately 90%, taking the 1002 cm^{-1} Phe mode as an internal standard) is indicative of Zn binding at the N_τ site of histidine side chains. Only 15−20% of this increase going from part A to part B of Figure 2 can be ascribed to the presence of tyrosinate (J. Dong and P. R. Carey, unpublished results). Further, the increase in the band intensity at 1278 cm^{-1} is indicative of a ring breathing mode of a histidine side chain ligated to Cu(II) at the N_π site. These results are consistent with recent findings that synthetic Aβ binds Cu(II) and Zn(II) via histidine residues (*27*, *29*, *33*). Our new data provide the bridge from the intensive studies on the synthetic protein to the intact, biologically relevant SP cores taken from AD brain.

Two modes of metal binding can be ruled out. There is no evidence of Cu(II)−, Co(II)−, or Fe(III)−tyrosinate binding (Figure 2B) which would give rise to characteristic intense bands, near 1504 and 1176 cm^{-1} (*9*, *11*, *12*). However, we cannot rule out the presence of Zn side chain interactions which could give rise to a tyrosinate. In another study, Miura et al. (*9*) showed that Cu(II) binding to a deprotonated peptide group [C(═O)N^-] gives rise to an intense Raman band near 1415 cm^{-1}. Since we do not detect this feature in the spectrum of the SP cores, we can conclude that Cu−amide$^-$ links are not prevalent.

The coexistence of methionine sulfoxide and Cu binding to histidines in SP cores creates the potential for coupled chemical reactions that generate neurotoxic H_2O_2. Free radical oxidative stress, particularly of neuronal proteins, is extensive in those AD brain areas in which Aβ is abundant. Recently, a series of experimental data have shown that Met35 acts as an electron donor for the reduction of synthetic Aβ-bound Cu^{II} to Cu^{I} (*31*, *34*−*36*):

$$\text{A}\beta\text{-MetS} + \text{Cu(L)}^{2+} = \text{A}\beta\text{-MetS}^{\bullet+} + \text{Cu(L)}^{+} \quad (1)$$

An abundance of antioxidant, like ascorbate, acting as a one-electron donor, provides for potential redox cycling via reactions 1−3 (*37*), where it is interesting to note that ref *37* deals with the generation of hydrogen peroxide by plaques:

$$\text{Cu(L)}^{+} + \text{O}_2 + 2\text{H}^{+} + \text{e} = \text{Cu(L)}^{2+} + \text{H}_2\text{O}_2 \quad (2)$$

$$\text{A}\beta\text{-MetS}^{\bullet+} + \text{e} = \text{A}\beta\text{-MetS} \quad (3)$$

Reaction 2 yields H_2O_2, while in reaction 3, the methionine cation radical is reduced back to methionine by cellular antioxidants. Methionine can be further oxidized to methionine sulfoxide in the presence of H_2O_2

$$\text{A}\beta\text{-MetS} + \text{H}_2\text{O}_2 = \text{A}\beta\text{-MetS=O} + \text{H}_2\text{O} \quad (4)$$

Overall, cellular reducing agents are consumed in reactions 2−4.

Metal Removal Leads to Structural Changes in the SP Cores. To test whether metal binding to SP cores is reversible, SP cores were treated with the chelator ethylenediaminetetraacetate (EDTA) (2.5 mM) overnight at pH 7.0 (Figure 2C). This resulted in a decrease in relative intensity of the 1278 cm^{-1} band, corroborating its assignment as a metal−ligand mode and suggesting that a significant portion of the His-bound Cu(II) was removed. Major intensity changes were not detected for the 1604 cm^{-1} Zn-associated mode. However, the band intensity at 1628 cm^{-1} (Figure 2B) is reduced upon chelation treatment, and is absent in synthetic fibrils. This band is assigned to the C═O group, either from the peptide backbone or from a Gln or Asn side chain, coordinated to an unidentified metal (*38*). Again, these data provide the extension from model studies to intact SP cores; previous *in vitro* studies showed that interactions of Zn and Cu with synthetic Aβ are reversible following chelation (*29*, *39*). Another notable change following chelation treatment is the broadening of the amide I and amide III features of the spectrum; e.g., for the amide I band, the bandwidths at half-height are 23 (fibrils), 22 (SP cores), and 26 cm^{-1} (EDTA-treated SP cores). This suggests that there

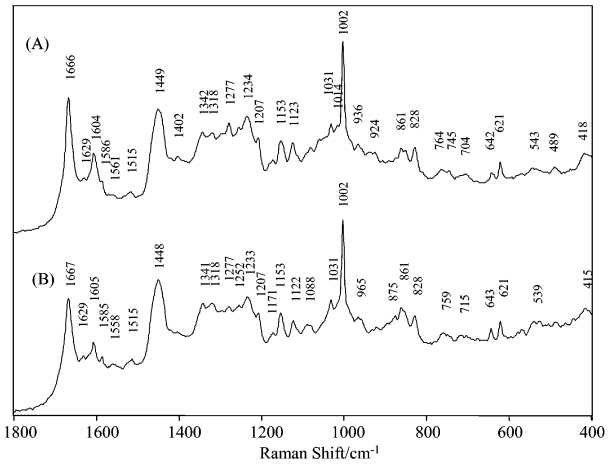

FIGURE 4: Raman spectra of (A) SP cores (case 93-319, female, 76 years old, 6 year history of AD) and (B) SP cores (case A91-441, female, 81 years old, 5 year history of AD).

is a greater heterogeneity, or loosening, of the β-structure upon metal ion removal with the peptide ψ and ϕ angles occupying a slightly larger region of Ramachandran space. Notably, homogenization of AD brains in buffers containing chelators liberates more Aβ than buffer alone, indicating that metal ions play an important role in maintaining the structural integrity of amyloid deposits (*40*).

Homogeneity of SP Cores from Different Sources. SP cores from the same AD brain, or from different AD brains (n = 3), appear to be remarkably similar. For example, Figure 4 compares the Raman spectra of a SP core plaque from a patient who died at 76 years of age (trace A, case 93-319, 6 year history of AD) to one from a patient who died at 81 years of age (trace B, case A91-441, 5 year history of AD). The spectra, with one or two minor exceptions, are essentially superimposable, demonstrating that the protein composition, conformation, and modifications are very similar in the two samples. Two intriguing differences are that in the trace from the brain from the person with a 5 year history of AD the His−Cu feature at 1278 cm^{-1} and the His−Zn feature at 1604 cm^{-1} are approximately 75 and 30% less intense (using the 1002 cm^{-1} Phe feature as an internal standard), respectively. This means that there is likely less Cu and Zn bound in the SP core sample that we examined from the brain from the person with a 5 year history of AD. More experiments are needed to confirm and quantify this observation.

Conclusion. Using Raman microscopy, we demonstrate for the first time that Aβ is the dominant component in SP cores and is present in a β-sheet, probably parallel β-helix conformation. Further, Cu(II) and Zn(II) are bound to histidine side chains within this structure. The loosening of SP cores following chelation treatment indicates that metal ions play an important structural role in SP cores, one that might be exploited to resolubilize amyloid. To this end, it has been found recently that oral administration of clioquinol (CQ), a specific bioavailable Cu/Zn chelator, to 21-month-old APP transgenic mice for 9 weeks reduces the amyloid burden by nearly 50% (*41*). Our results also explain how desferrioxamine, a chelator with affinities for Cu(II), Fe(III), Zn(II), and Al(III), may have acted to inhibit the progression of AD in an earlier clinical trial (*42*). Thus, the work presented here underscores the potential for the use of chelators as therapeutic agents in AD. In a more general sense, we have shown that Raman microscopy offers a promising means for eliciting detailed chemical information from insoluble microscopic neural inclusions.

REFERENCES

1. Glenner, G. G., and Wong, C. W. (1984) *Biochem. Biophys. Res. Commun. 120*, 885−890.
2. Masters, C. L., Simms, G., Weinman, N. A., Multhaup, G., McDonald, B. L., and Beyreuther, K. (1985) *Proc. Natl. Acad. Sci. U.S.A. 82*, 4245−4249.
3. Roher, A. E., Lowenson, J. D., Clarke, S., Wolkow, C., Wang, R., Cotter, R. J., Reardon, I. M., Zurcher-Neely, H. A., Heinrikson, R. L., Ball, M. J., and Greenberg, B. D. (1993) *J. Biol. Chem. 268*, 3072−3083.
4. Atwood, C. S., Martins, R. N., Smith, M. A., and Perry, G. (2002) *Peptides 23*, 1343−1350.
5. Merz, P. A., Wisniewski, H. M., Somerville, R. A., Bobin, S. A., Masters, C. L., and Iqbal, K. (1983) *Acta Neuropathol. 60*, 113−124.
6. Kirschner, D. A., Abraham, C., and Selkoe, D. J. (1986) *Proc. Natl. Acad. Sci. U.S.A. 83*, 503−507.
7. Glenner, G. G. (1981) *Prog. Histochem. Cytochem. 13*, 1−37.
8. Lansbury, P. T., Jr., Costa, P. R., Griffiths, J. M., Simon, E. J., Auger, M., Halverson, K. J., Kocisko, D. A., Hendsch, Z. S., Ashburn, T. T., and Spencer, R. G. (1995) *Nat. Struct. Biol. 2*, 990−998.
9. Miura, T., Suzuki, K., Kohata, N., and Takeuchi, H. (2000) *Biochemistry 39*, 7024−7031.
10. Miura, T., Satoh, T., Hori-i, A., and Takeuchi, H. (1998) *J. Raman Spectrosc. 29*, 41−47.
11. Suzuki, K., Miura, T., and Takeuchi, H. (2001) *Biochem. Biophys. Res. Commun. 285*, 991−996.
12. Miura, T., Suzuki, K., and Takeuchi, H. (2001) *J. Mol. Struct. 598*, 79−84.
13. Hashimoto, S., Ono, K., and Takeuchi, H. (1998) *J. Raman Spectrosc. 29*, 969−975.
14. Hashimoto, S., Ohsaka, S., Takeuchi, H., and Harada, I. (1989) *J. Am. Chem. Soc. 111*, 8926−8927.
15. Hasegawa, K., Ono, T., and Noguchi, T. (2002) *J. Phys. Chem. A 106*, 3390.
16. Que, L., Jr. (1983) *Coord. Chem. Rev. 50*, 73−108.
17. DeWitt, D. A., Perry, G., Cohen, M., Doller, C., and Silver, J. (1998) *Exp. Neurol. 149*, 329−340.
18. Cras, P., Kawai, M., Lowery, D., Gonzalez-DeWhitt, P., Greenberg, B., and Perry, G. (1991) *Proc. Natl. Acad. Sci. U.S.A. 88*, 7552−7556.
19. Altose, M. D., Zheng, Y., Dong, J., Palfey, B. A., and Carey, P. R. (2001) *Proc. Natl. Acad. Sci. U.S.A. 98*, 3006−3011.
20. Carey, P. R. (1982) *Biochemical Applications of Raman and Resonance Raman Spectroscopies*, Academic Press, New York.
21. Raso, S. W., Clark, P. L., Haase-Pettingell, C., King, J., and Thomas, G. J., Jr. (2001) *J. Mol. Biol. 307*, 899−911.
22. Sunde, M., Serpell, L. C., Bartlam, M., Fraser, P. E., Pepys, M. B., and Blake, C. C. F. (1997) *J. Mol. Biol. 273*, 729−739.
23. Antzutkin, O. N., Balbach, J. J., Leapman, R. D., Rizzo, N. W., Reed, J., and Tycko, R. (2000) *Proc. Natl. Acad. Sci. U.S.A. 97*, 13045−13050.
24. Harada, I., and Takeuchi, H. (1986) Raman and ultraviolet resonance Raman spectra of proteins and related compounds, in *Advances in Infrared and Raman Spectroscopy*, *Vol. 13, Spectroscopy of Biological Systems* (Clark, R. J. H., and Hester, R. E., Eds.) pp 113−175, Wiley, Chichester, U.K.
25. Butterfield, D. A., and Kanski, J. (2002) *Peptides 23*, 1299−1309.
26. Lovell, M. A., Robertson, J. D., Teesdale, W. J., Campbell, J. L., and Markesbery, W. R. (1998) *J. Neurol. Sci. 158*, 47−52.
27. Atwood, C. S., Scarpa, R. C., Huang, X., Moir, R. D., Jones, W. D., Fairlie, D. P., Tanzi, R. E., and Bush, A. I. (2000) *J. Neurochem. 75*, 1219−1233.
28. Bush, A. I., Pettingell, W. H. J., Paradis, M. D., and Tanzi, R. E. (1994) *J. Biol. Chem. 269*, 12152−12158.
29. Atwood, C. S., Huang, X., Moir, R. D., Bacarra, N. M., Romano, D., Tanzi, R. E., and Bush, A. I. (1998) *J. Biol. Chem. 273*, 12817−12826.
30. Cuajungco, M. P., Goldstein, L. E., Nunomura, A., Smith, M. A., Lim, J. T., Atwood, C. S., Huang, X., Farrag, Y. W., Perry, G., and Bush, A. I. (2000) *J. Biol. Chem. 275*, 19439−19442.

31. Huang, X., Cuajungco, M. P., Atwood, C. S., Hartshorn, M. A., Tyndall, J., Hanson, G. R., Stokes, K. C., Multhaup, G., Goldstein, L. E., Scarpa, R. C., Saunders, A. J., Lim, J., Moir, R. D., Glabe, C., Bowden, E. F., Masters, C. L., Fairlie, D. P., Tanzi, R. E., and Bush, A. I. (1999) *J. Biol. Chem. 274*, 37111−37116.
32. Rottkamp, C. A., Raina, A. K., Zhu, X., Gaier, E., Bush, A. I., Atwood, C. S., Chevion, M., Perry, G., and Smith, M. A. (2001) *Free Radical Biol. Med. 30*, 447−450.
33. Curtain, C. C., Ali, F., Volitakis, I., Cherny, R. A., Norton, R. S., Beyreuther, K., Barrow, C. J., Masters, C. L., Bush, A. I., and Barnham, K. J. (2001) *J. Biol. Chem. 276*, 20466−20473.
34. Schoneich, C. (2002) *Arch. Biochem. Biophys. 397*, 370−376.
35. Varadarajan, S., Kanski, J., Aksenova, M., Lauderback, C., and Butterfield, D. A. (2001) *J. Am. Chem. Soc. 123*, 5625−5631.
36. Varadarajan, S., Yatin, S., Kanski, J., Jahanshahi, F., and Butterfield, D. A. (1999) *Brain Res. Bull. 50*, 133−141.
37. Opazo, C., Huang, X., Cherny, R., Moir, R., Roher, A., White, A., Cappai, R., Masters, C., Tanzi, R., Inestrosa, N., and Bush, A. (2002) *J. Biol. Chem. 29*, 40302−40308.
38. Kaneda, A., and Martell, A. E. (1975) *J. Coord. Chem. 4*, 137−151.
39. Huang, X., Atwood, C. S., Moir, R. D., Hartshorn, M. A., Vonsattel, J. P., Tanzi, R. E., and Bush, A. I. (1997) *J. Biol. Chem. 272*, 26464−26470.
40. Cherny, R. A., Legg, J. T., McLean, C. A., Fairlie, D. P., Huang, X., Atwood, C. S., Beyreuther, K., Tanzi, R. E., Masters, C. L., and Bush, A. I. (1999) *J. Biol. Chem. 274*, 23223−23228.
41. Cherny, R. A., Atwood, C. S., Xilinas, M. E., Gray, D. N., Jones, W. D., McLean, C. A., Barnham, K. J., Volitakis, I., Fraser, F. W., Kim, Y., Huang, X., Goldstein, L. E., Moir, R. D., Lim, J. T., Beyreuther, K., Zheng, H., Tanzi, R. E., Masters, C. L., and Bush, A. I. (2001) *Neuron 30*, 665−676.
42. Crapper-McLachlan, D. R., Dalton, A. J., Kruck, T. P., Bell, M. Y., Smith, W. L., Kalow, W., and Andrews, D. F. (1991) *Lancet 337*, 1304−1308.
43. Wetzel, R. (2002) *Structure 10*, 1031−1036.
44. Overman, S. A., and Thomas, G. J., Jr. (1999) Raman markers of nonaromatic side chains in an α-helix assembly: Ala, Asp, Glu, Gly, Ile, Leu, Lys, Ser, and Val residues of phage *fd* subunits, *Biochemistry 38*, 4018−4027.

BI0272151